

π and σ -Phenylethynyl Radicals and Their Isomers *o*-, *m*-, and *p*-Ethynylphenyl: Structures, Energetics, and Electron Affinities

Raj K. Sreeruttun,^{†,‡} Ponnadurai Ramasami,[†] Chaitanya S. Wannere,[‡]
Andrew C. Simmonett,[‡] and Henry F. Schaefer, III^{*‡}

Department of Chemistry, Faculty of Science, University of Mauritius, Republic of Mauritius, and
Center for Computational Chemistry, University of Georgia, Athens, Georgia 30602

Received: August 7, 2007; In Final Form: January 2, 2008

Molecular structures, energetics, vibrational frequencies, and electron affinities are predicted for the phenylethynyl radical and its isomers. Electron affinities are computed using density functional theory, namely, the B3LYP, BLYP, B3LYP, BP86, BPW91, and B3PW91 functionals, employing the double- ζ plus polarization DZP++ basis set; this level of theory is known to perform well for the computation of electron affinities. Furthermore, ab initio computations employing perturbation theory, coupled cluster with single and double excitations [CCSD], and the inclusion of perturbative triples [CCSD(T)] are performed to determine the relative energies of the isomers. These higher level computations are performed with the correlation consistent family of basis sets cc-pVXZ ($X = D, T, Q, 5$). Three electronic states are probed for the phenylethynyl radical. In C_{2v} symmetry, the out-of-plane (2B_1) radical is predicted to lie about 10 kcal/mol below the in-plane (2B_2) radical by DFT methods, which becomes 9.4 kcal/mol with the consideration of the CCSD(T) method. The energy difference between the lowest π and σ electronic states of the phenylethynyl radical is also about 10 kcal/mol according to DFT; however, CCSD(T) with the cc-pVQZ basis set shows this energy separation to be just 1.8 kcal/mol. The theoretical electron affinities of the phenylethynyl radical are predicted to be 3.00 eV (B3LYP/DZP++) and 3.03 eV (CCSD(T)/DZP++//MP2/DZP++). The adiabatic electron affinities (EA_{ad}) of the three isomers of phenylethynyl, that is, the *ortho*-, *meta*-, and *para*-ethynylphenyl, are predicted to be 1.45, 1.40, and 1.43 eV, respectively. Hence, the phenylethynyl radical binds an electron far more effectively than the three other radicals studied. Thermochemical predictions, such as the bond dissociation energies of the aromatic and ethynyl C–H bonds and the proton affinities of the phenylethynyl and ethynylphenyl anions, are also reported.

I. Introduction

The phenylethynyl radical, which has been described as a π radical in both the gas phase and solution,^{1,2} is unlike ethynyl, HC≡C•, and cyanogen, N≡C•, which are σ radicals.^{3,4} Kasai and McBay² (1984) examined the crossing of the σ and π electronic states in the phenylethynyl radical, resulting from the mixing of the π_z orbital of the ethynyl moiety and the E_{1a} π orbital of the phenyl group. An antisymmetric interaction of these two orbitals produces a π orbital (highest occupied semi-filled orbital, the singly occupied molecular orbital, i.e., SOMO) which is energetically less stable than the nonbonding σ orbital of the ethynyl part. In simpler terms, there is electron transfer from the highest occupied π orbital of the phenyl group into the σ nonbonding orbital of the ethynyl system.

Generated by the photolysis of 1-iodo-2-phenylacetylene (PhC≡C–I), the phenylethynyl radical has been investigated for its stability and reactions by Martelli, Spagnolo, and Tiecco⁵ (1970). The phenylethynyl radical undergoes homolytic aromatic substitution with aromatic compounds to give substituted products and was found to be electrophilic toward substituted benzene molecules by Martelli. However, the electrophilicity of the radical toward aromatic substances was concluded to be

less pronounced at the *ortho* position with monosubstituted benzene derivatives. The reaction of cuprous phenylacetylide with aryl iodide was also considered, however this led to the description of the phenylethynyl radical as a σ radical.⁵

Casanova, Geisel, and Morris⁶ (1969) studied the thermal stability of the phenylethynyl anion (PhC≡C[−]). The thermal rearrangement of this anion with respect to phenylethyne-1-¹³C was assumed to be a first-order rearrangement ($\Delta H \geq 37.4$ kcal/mol) in polar solvents.



Recently, Bölm, Pafík, and Exner⁷ (2006) studied the acidities of *meta*- and *para*-substituted phenylethyne (phenylacetylene) and correlated these acidities with Hammett equation calculations with respect to benzoic acid derivatives. The gas-phase acidities of the substituted phenylethyne and the Hammett constants associated with isodesmic reactions of the substituted phenylethyne compounds yield a reasonable linear free energy relationship. However, a failure in the Hammett equation has been observed in some cases, especially in neutral molecules.^{8,9}

A detailed analysis of the pyrolysis products of phenylethyne was carried out in 1995 by Hofmann et al. in which reactive intermediates such as radicals and carbenes were considered.¹⁰ In addition to the phenylethynyl free radical, the three isomeric *ortho*-, *meta*-, and *para*-ethynylphenyl radicals ($\cdot\text{C}_6\text{H}_4\text{C}\equiv\text{CH}$) were identified. Very recently, the C₂ + C₆H₆ reaction has been

* To whom correspondence should be addressed. E-mail: hfs@uga.edu.
Tel: (706) 542 7172. Fax: (706) 542 0406.

[†] University of Mauritius.

[‡] University of Georgia.

studied in crossed molecular beams by Kaiser,¹¹ yielding the phenylethynyl radical. The aforementioned isomeric ethynylphenyl radicals were not observed; a fact that was attributed to the short lifetime of the crucial transition state that would require a sufficient lifetime to undergo rearrangement to yield the thermodynamically favored ethynylphenyl moieties.

The present research begins with the computation of the hitherto unknown electron affinity of the phenylethynyl radical. For clarity, we define the adiabatic electron affinity as the energy difference between the total energy at the geometry-optimized radical and the total energy at the corresponding geometry-optimized anion

$$\text{Adiabatic electron affinity, } EA_{\text{ad}} = E(\text{optimized radical}) - E(\text{optimized anion}) \quad (2)$$

The zero-point vibrational energy (ZPVE) corrected electron affinities are determined by appending the ZPVE, from harmonic vibrational frequencies, for each species to the corresponding total energies

$$\text{ZPVE-corrected electron affinity} = [E(\text{optimized radical}) + \text{ZPVE}_{\text{radical}}] - [E(\text{optimized anion}) + \text{ZPVE}_{\text{anion}}] \quad (3)$$

Further, the energy difference ($\Delta E_{\sigma-\pi}$) between the σ and π radical states has been investigated.

$$\Delta E_{\sigma-\pi} = E(\text{optimized } \sigma \text{ radical}) - E(\text{optimized } \pi \text{ radical}) \quad (4)$$

This research also reports the bond dissociation energies of the ethynyl and the aromatic C–H bonds in phenylethyne.

II. Theoretical Details

Electron affinities were computed using density functional theory, which has been shown to be an inexpensive and effective method for the prediction of this quantity.¹² The pure DFT functionals utilized are as follows: Becke's exchange functional^{13,14} with the Lee–Yang–Parr nonlocal correlation functional¹⁵ (BLYP), the same exchange functional with the correlation functional of Perdew¹⁶ (BP86), and BPW91 which also uses Becke exchange with the PW91 correlation functional. In addition to the pure DFT methods, we employed BHLYP, which mixes Hartree–Fock exchange with Becke's 1988 exchange functional,^{13,14} and the popular combination of the three-parameter Becke functional¹⁷ with the Lee–Yang–Parr nonlocal correlation functional (B3LYP). The basis set used was Dunning's 1970 double- ζ basis set with polarization and diffuse functions, denoted DZP++.¹² These sets were constructed by augmenting the Huzinaga–Dunning^{18–20} sets of contracted Gaussian functions with one set of p polarization functions for each H atom and one set of d polarization functions for each C atom. [$\alpha_p(\text{H}) = 0.75$, $\alpha_d(\text{C}) = 0.75$]. To describe anions, the basis was further augmented with diffuse functions. Diffuse functions were determined in an even-tempered fashion according to the prescription of Lee and Schaefer²¹

$$\alpha_{\text{diffuse}} = \left(\frac{\alpha_1 + \alpha_2}{\alpha_3} \right) \alpha_1 \quad (5)$$

where α_1 , α_2 , and α_3 are the three smallest Gaussian orbital exponents of the s- or p-type primitive functions of a given atom ($\alpha_1 < \alpha_2 < \alpha_3$). This procedure yields $\alpha_s(\text{H}) = 0.04415$; $\alpha_s(\text{C}) = 0.04302$, $\alpha_p(\text{C}) = 0.03629$. The final contraction scheme for the DZP++ basis set H(5s1p/3s1p) and C(10s6p1d/5s3p1d). For the four radicals considered here, the DZP++ basis set comprises 182 basis functions.

Relative isomerization energies are more difficult to pinpoint and were therefore refined by the consideration of ab initio single point energies via the OPT1,²² OPT2,²² and ZAPT2²³ variants of restricted open shell perturbation theory²⁴ and the more rigorous coupled-cluster methods with singles and doubles [CCSD], and non-iterative triples corrections [CCSD(T)]. These energy refinements were executed with Dunning's correlation consistent family of basis sets^{25–27} (cc-pVXZ, X = D, T, Q, 5); the largest basis set includes 1003 basis functions for the phenylethynyl radical.

Unrestricted DFT methods were employed for the open shell systems. The Gaussian94²⁸ and Gaussian03²⁹ programs were used to carry out the computations, which include a fine grid (75 302) as the default for evaluating integrals numerically, and the tight (10^{-8} Hartrees) specification as the default for SCF convergence. The OPT1, OPT2, and ZAPT2 computations were facilitated by the MPQC software package,³⁰ while the Molpro suite of programs³¹ provided the coupled-cluster results.

III. Results and Discussions

A. Geometrical Structures. The structure of the phenylethynyl radical has been deduced to be of C_{2v} symmetry from experiment.^{1,2} In our research, the geometry of the phenylethynyl radical has been optimized within both C_s and C_{2v} symmetry. The BHLYP/DZP++ and B3LYP/DZP++ methods predict a C_{2v} phenylethynyl radical (2B_1 state). In contrast, the radical optimizes to C_s (${}^2A'$) symmetry with the BLYP, BP86, BPW91, and B3PW91 functionals and the same basis set. In the latter four cases, their C–C \equiv C bond angles are between 165° and 171° , that is, nearly linear. The geometries optimized by the HF and MP2 methods with the DZP++ basis set agree with the qualitative experimental C_{2v} structure of the phenylethynyl radical.

Figure 1 shows the optimized structures of the phenylethynyl radical and anion predicted by the different theoretical methods. If the B3LYP/DZP++ results are compared, then it is found that the ethynyl bond length in the phenylethynyl radical (1.290 Å) is longer than that for the phenylethynyl anion (1.261 Å). Further, the C–C \equiv C bond length in the anion (1.424 Å) is longer than that in the radical (1.404 Å). Thus, the bond order of the ethynyl bond of the radical appears to be less than that of the anion.

With the BLYP/DZP++ method, the 2B_1 state of the phenylethynyl radical is a transition state rather than a genuine minimum on the potential energy surface. An imaginary vibrational frequency is predicted, reflecting the bending of the ethynyl moiety in the radical. The ethynyl group bends to an equilibrium angle ca. 167° (BLYP/DZP++). The bending of the ethynyl group with the DZP++ basis sets was also observed for the propynyl and propargyl systems.⁴

The energy difference between the C_{2v} transition state and the optimized C_s phenylethynyl radical with the different DFT methods is shown in Table 1. A rather low energy difference is observed in these cases. Indeed, these energy differences are so small (< 1 kcal/mol) that an EPR experiment^{1,2} may not easily distinguish between the C_{2v} and C_s equilibrium geometries. In either case, the vibrationally averaged structure will reflect C_{2v} symmetry.

B. C₂H Radical as a Benchmark. As a point of calibration, the adiabatic electron affinity of the ethynyl radical is predicted to be (2.92, 2.93, 3.07, 3.10, 2.93, 3.00) eV by the (BHLYP, BLYP, B3LYP, BP86, BPW91, B3PW91) functionals using the DZP++ basis set.³² These results all compare favorably with the experimental value of 2.969 ± 0.006 eV.³³

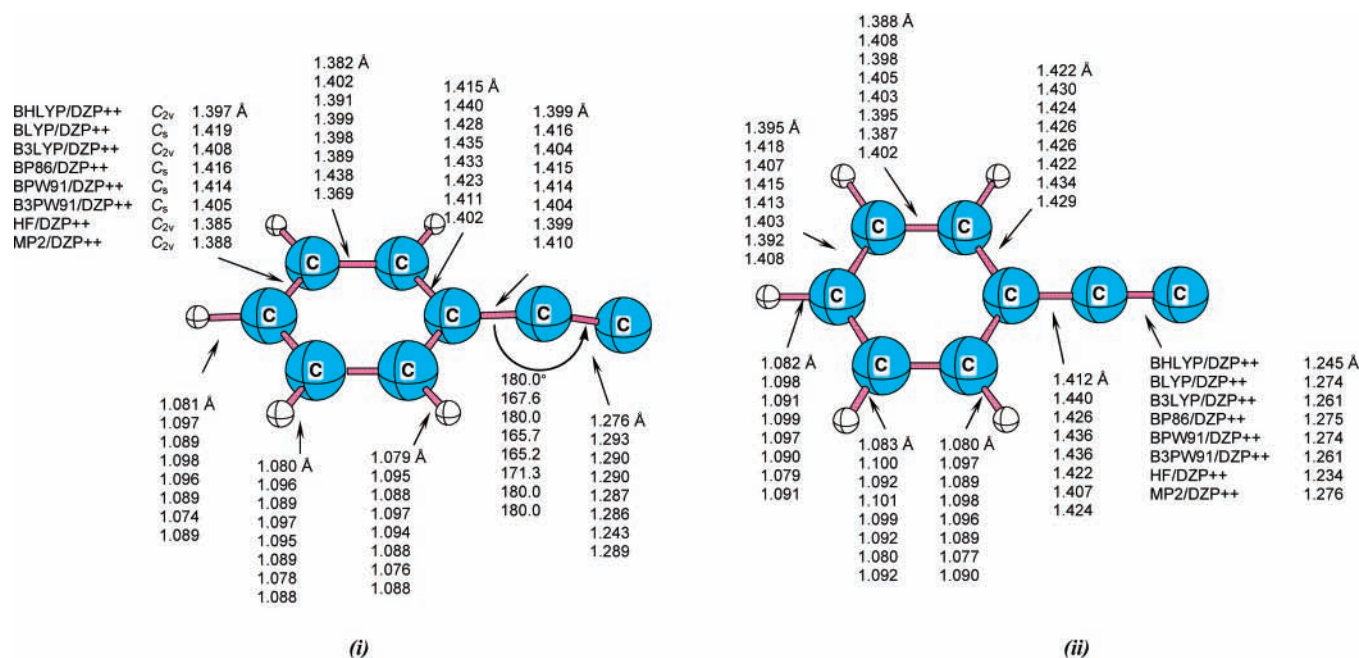


Figure 1. Optimized geometries of the phenylethynyl radical (i) and anion (ii) in the gas phase. All the methods employed predict a C_{2v} geometry for the phenylethynyl anion.

TABLE 1: Energy Differences between the C_{2v} Transition State and the Optimized C_s Equilibrium Geometry of the Phenylethynyl Radical

methods	radical (planar)			radical (bent ethynyl)			$\Delta E (C_{2v}-C_s)$ kcal/mol
			E_{elec} (Hartrees)			E_{elec} (Hartrees)	
BLYP/DZP++	C_{2v}	2B_1	-307.59238	C_s	${}^2A'$	-307.59305	0.42
BP86/DZP++	C_{2v}	2B_1	-307.71146	C_s	${}^2A'$	-307.71263	0.74
BPW91/DZP++	C_{2v}	2B_1	-307.67981	C_s	${}^2A'$	-307.68127	0.92
B3PW91/DZP++	C_{2v}	2B_1	-307.59711	C_s	${}^2A'$	-307.59726	0.09

TABLE 2: Theoretical Adiabatic Electron Affinities (EA) for the Phenylethynyl Radical^a

methods	radical				anion				
				E_{elec} (Hartrees)				E_{elec} (Hartrees)	EA (eV)
DFT	BHLYP/DZP++	C_{2v}	2B_1	-307.53787	C_{2v}	1A_1	-307.63896	2.75 (2.75)	
	BLYP/DZP++	C_s	${}^2A'$	-307.59305	C_{2v}	1A_1	-307.69765	2.85 (2.86)	
	B3LYP/DZP++	C_{2v}	2B_1	-307.72259	C_{2v}	1A_1	-307.83267	3.00 (3.00)	
	BP86/DZP++	C_s	${}^2A'$	-307.71263	C_{2v}	1A_1	-307.82565	3.08 (3.09)	
	BPW91/DZP++	C_s	${}^2A'$	-307.68127	C_{2v}	1A_1	-307.78941	2.94 (2.95)	
	B3PW91/DZP++	C_s	${}^2A'$	-307.59726	C_{2v}	1A_1	-307.70762	3.00 (3.01)	
ab initio	HF/DZP++	C_{2v}	2B_1	-305.76955	C_{2v}	1A_1	-305.82193	1.43	
	HF/cc-pVDZ	C_{2v}	2B_1	-305.74545	C_{2v}	1A_1	-305.78678	1.12	
	HF/cc-pVTZ	C_{2v}	2B_1	-305.81858	C_{2v}	1A_1	-305.84870	0.82	
	HF/cc-pVQZ	C_{2v}	2B_1	-305.83701	C_{2v}	1A_1	-305.88801	1.39	
	MP2/DZP++	C_{2v}	2B_1	-306.70022	C_{2v}	1A_1	-306.85148	4.12	
	MP2/cc-pVDZ	C_{2v}	2B_1	-306.67765	C_{2v}	1A_1	-306.81689	3.79	
	MP2/cc-pVTZ	C_{2v}	2B_1	-306.95988	C_{2v}	1A_1	-307.10684	4.00	
	CCSD/DZP++//MP2/DZP++	C_{2v}	2B_1	-306.78227	C_{2v}	1A_1	-306.88723	2.86	
	CCSD(T)/DZP++//MP2/DZP++	C_{2v}	2B_1	-306.82892	C_{2v}	1A_1	-306.94044	3.03	

^a The ZPVE-corrected electron affinities are listed in parentheses.

C. Electron Affinity of the Phenylethynyl Radical. The electron affinity of phenylethynyl radical is not known from experiment. A rough estimate for the electron affinity (EA) of the phenylethynyl radical may be found from the following equation:^{34,35}

$$EA(\text{PhCC}) = D(\text{PhCC-H}) + IP(\text{H}) - \Delta H_{\text{acid}} \quad (6)$$

where, ΔH_{acid} is the enthalpy change for acid dissociation in the *gas phase* (372 kcal/mol),³⁵ $IP(\text{H})$ is the ionization potential for hydrogen (314 kcal/mol),³⁴ and $D(\text{PhCC-H})$ is the bond dissociation energy of the $\equiv\text{C-H}$ bond in phenylethyne. The

latter value is, however, not available experimentally and has been variously estimated to be 132 ± 5 kcal/mol¹⁰ or ≥ 125 kcal/mol.³⁶ For comparison, the bond dissociation energy of the C-H bond in acetylene is known to be 133.2 ± 0.07 kcal/mol.³⁷ If the bond dissociation of the C-H bond in acetylene is considered to be 133.2 ± 0.07 kcal/mol in eq 6, then the electron affinity of the phenylethynyl radical is roughly approximated to be 3.26 eV.

Table 2 presents the total energies of the phenylethynyl radical and anion optimized by the different quantum chemical methods and, more importantly, the adiabatic electron affinity of the phenylethynyl radical. The majority of the computational

TABLE 3: Energy Differences between the Ground and Low-lying States of the Phenylethynyl Radical

methods	2B_1 state π radical (GS) (Hartrees)	2A_1 state σ radical (Hartrees)	2B_2 state π radical (Hartrees)	ΔE (2A_1 - 2B_1) (kcal/mol)	ΔE (2B_2 - 2B_1) (kcal/mol)
HF/DZP++	-305.76955	-305.76849	-305.75437	0.7	9.5
BHLYP/DZP++	-307.53787	-307.52280	-307.52204	9.5	9.9
B3LYP/DZP++	-307.72260	-307.70644	-307.70530	10.1	10.9
BLYP/DZP++ ^a	-307.59238	-307.57404	-307.57377	11.5	11.7
BP86/DZP++ ^a	-307.71146	-307.69647	-307.69385	9.4	11.1
BPW91/DZP++ ^a	-307.67981	-307.66683	-307.66274	8.1	10.7
B3PW91/DZP++ ^a	-307.59711	-307.58555	-307.58105	7.3	10.1
OPT1/DZP++	-306.74600	-306.74593	-306.73186	0.1	8.9
OPT1/cc-pVDZ ^b	-306.72129	-306.71908	-306.70573	-1.4	8.4
OPT1/cc-pVTZ ^b	-307.00264	-307.00004	-306.98616	-1.6	8.7
OPT1/cc-pVQZ ^b	-307.09593	-307.09324	-307.07917	-1.7	8.8
OPT1/cc-pV5Z ^b	-307.12883	-307.12608	-307.11195	-1.7	8.9
OPT2/DZP++	-306.73673	-306.74050	-306.72382	-2.4	8.1
OPT2/cc-pVDZ ^b	-306.71577	-306.70980	-306.69762	-3.7	7.6
OPT2/cc-pVTZ ^b	-306.99652	-306.98994	-306.97727	-4.1	8.0
OPT2/cc-pVQZ ^b	-307.08967	-307.08294	-307.07008	-4.2	8.1
OPT2/cc-pV5Z ^b	-307.12255	-307.11571	-307.10280	-4.3	8.1
ZAPT2/DZP++	-306.735792	-306.73866	-306.72320	-1.8	7.9
ZAPT2/cc-pVDZ ^b	-306.71393	-306.70886	-306.69696	-3.2	7.5
ZAPT2/cc-pVTZ ^b	-306.99459	-306.98887	-306.97649	-3.6	7.8
ZAPT2/cc-pVQZ ^b	-307.08773	-307.08183	-307.06928	-3.7	7.9
ZAPT2/cc-pV5Z ^b	-307.12061	-307.11460	-307.10199	-3.8	7.9
CCSD/cc-pVDZ ^b	-306.75983	-306.76332	-306.75048	2.2	8.1
CCSD/cc-pVTZ ^b	-307.02095	-307.02459	-307.01112	2.3	8.5
CCSD/cc-pVQZ ^b	-307.09951	-307.10301	-307.08936	2.2	8.6
CCSD(T)/cc-pVDZ ^b	-306.80977	-306.81286	-306.79891	1.9	8.8
CCSD(T)/cc-pVTZ ^b	-307.09206	-307.09503	-307.08034	1.9	9.2
CCSD(T)/cc-pVQZ ^b	-307.17601	-307.17889	-307.16394	1.8	9.4

^a The C_{2v} geometries with these four functionals are transition states, with energies less than 1 kcal/mol above the analogous optimum C_s geometry energies. ^b Single-point energies at the B3LYP/DZP++ equilibrium geometries.

methods (DFT) predict electron affinities in qualitative agreement with the crude electron affinity estimated with the above-discussed experimental assumptions (3.26 eV); the electron affinity for the phenylethynyl radical at the B3LYP/DZP++ method is 3.00 eV. Second-order Møller–Plesset perturbation theory (MP2) predicts electron affinities about 1 eV larger than the DFT methods; however, the CCSD(T)/DZP++//MP2/DZP++ electron affinity of 3.03 eV is in good agreement with those emanating from DFT. The propensity of MP2 to overestimate the correlation energy is most likely the cause of the large electron affinity. Likewise, Hartree–Fock theory underestimates the electron affinity relative to coupled-cluster theory due to its neglect of correlation energy. The anticipated accurate performance of DFT is largely due to fortuitous cancellation of error for the anion and the neutral.¹²

D. π and σ Radicals of Phenylethynyl. The $\tilde{A}^2\Pi \leftarrow \tilde{X}^2\Sigma^+$ ($C_{\infty v}$) electronic excitation energy of the ethynyl radical ($\text{HC}\equiv\text{C}\cdot$) is 10.6 kcal/mol.³⁸ Further, the electronic absorption and emission spectra of the valence singlet and triplet $\pi \rightarrow \pi^*$ excited states of phenylethyne have been studied recently by means of a multiconfigurational second-order perturbation method and its multistate extension.³⁹ Recently, Scheer and Burrow⁴⁰ studied the temporary anion states arising when an electron attaches to the antibonding π orbitals (π^*) in phenylethyne and related systems. However, the electronic transitions in the phenylethynyl radical have not been explored in the laboratory.

The phenylethynyl radical is a π radical with a 2B_1 ground state, implying that there is a singly occupied molecular orbital (SOMO) of π nature. Table 3 shows the relative energies of the various electronic states. All the DFT methods support the fact that the phenylethynyl radical is a π system.

The BHLYP/DZP++ and B3LYP/DZP++ methods predict a 2B_1 π radical whereas the other functionals predict a slightly

bent (C_s symmetry) radical. The phenylethynyl radical optimized by the BLYP, BP86, BPW91, and B3PW91 functionals with the DZP++ basis set has a ${}^2A'$ ground state, with a half-filled π SOMO. The ${}^2A'$ symmetry state correlates to 2B_1 in C_{2v} symmetry and arises from bending the ethynyl group perpendicular to the plane of the ring.

The energy difference ($\Delta E_{\sigma-\pi}$) between the optimized 2B_1 π radical state and optimized 2A_1 σ -radical state is an important quantity for radical chemistry. Table 3 shows the theoretical $\Delta E_{\sigma-\pi}$ values for the phenylethynyl radical with both DFT and ab initio methods. The B3LYP/DZP++ method predicts a $\Delta E_{\sigma-\pi}$ value of 10.1 kcal/mol; however, we investigated the reliability of this number in a hierarchical way by considering more rigorous levels of theory. These ab initio computations were performed at the DFT geometries, as it is widely understood that the geometric parameters from density functional approaches are generally reliable.¹²

The three restricted open shell perturbation theories considered here, OPT1, OPT2, and ZAPT2, all yielded the anomalous result that the σ radical is in fact lower in energy than the out-of-plane π radical; this result is insensitive to the choice of basis set. A more rigorous treatment of correlation through coupled-cluster theory restores the correct order, with the 2B_1 state lying 2.2 kcal/mol below the 2A_1 state. This separation decreases to 1.8 kcal/mol with the inclusion of perturbative triple excitations. We can conclude that DFT provides the correct state orderings, although the magnitude of the separation of these two states is overestimated by about 8 kcal/mol.

The ${}^2\Pi$ state of the parent C_2H molecule is doubly degenerate. This means that for phenylethynyl radical there are two low-lying π states, one with the singly occupied π orbital out-of-plane (2B_1), and the other in-plane (2B_2). In C_{2v} symmetry, the higher lying π state is of 2B_2 symmetry. Total and relative energies for this second π state are also reported in Table 3.

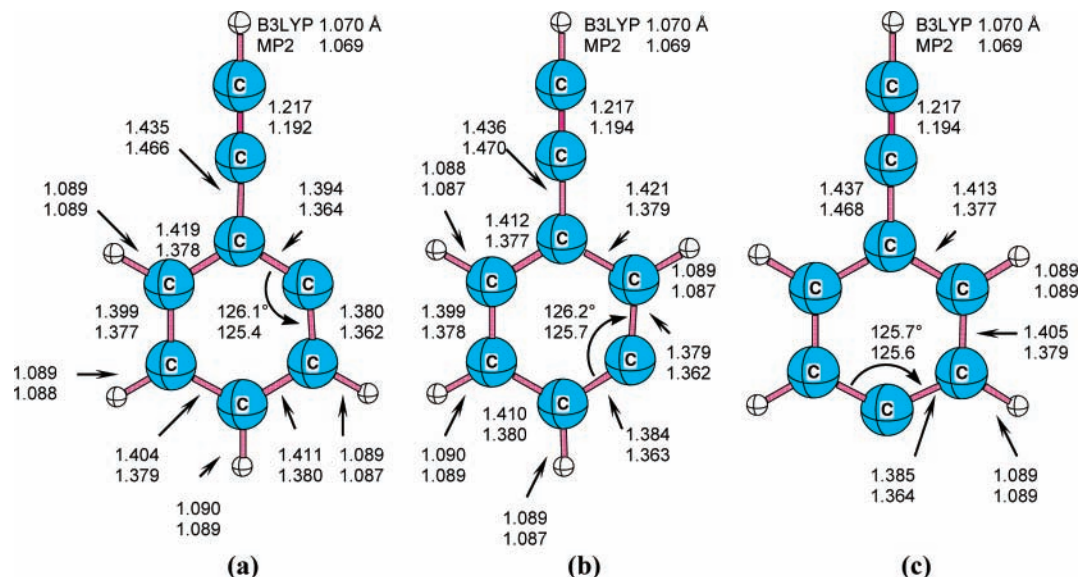


Figure 2. Optimized geometries of the *ortho*- (a), *meta*- (b), and *para*- (c) ethynylphenyl radicals with the B3LYP and MP2 methods in conjunction with the DZP++ basis sets. The geometries of (a), (b), and (c) are C_s , C_s , and C_{2v} , respectively.

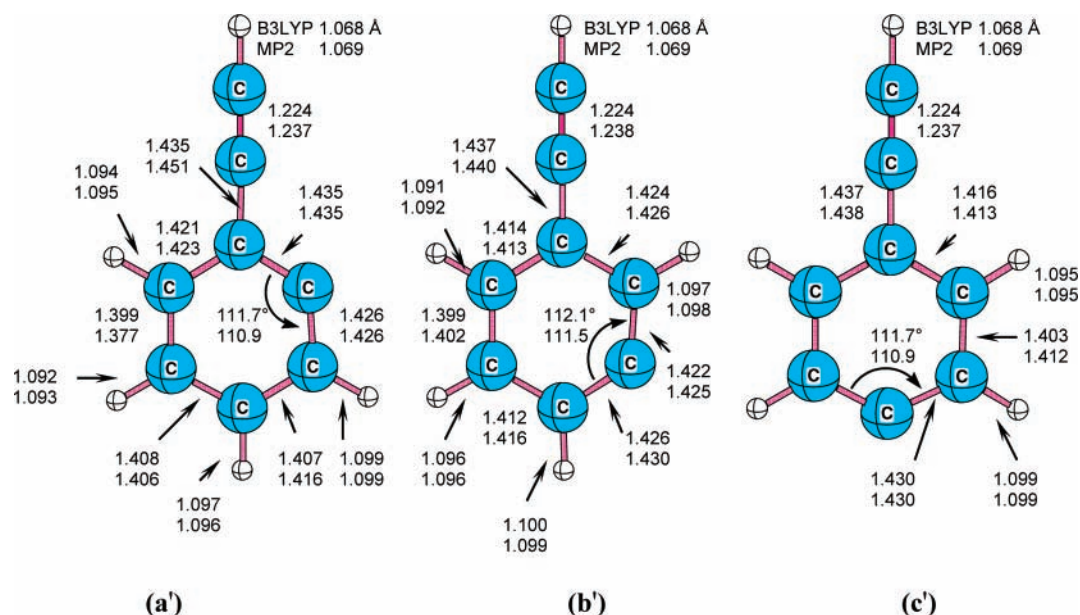


Figure 3. Optimized geometries of the *ortho*- (a'), *meta*- (b'), and *para*- (c') ethynylphenyl anions with the B3LYP and MP2 methods in conjunction with the DZP++ basis sets. The geometries of (a'), (b'), and (c') are C_s , C_s , and C_{2v} , respectively.

DFT predicts the separation of these two states to be about 11 kcal/mol, which compares quite favorably with the CCSD(T)/cc-pVQZ value of 9.4 kcal/mol.

E. Radical Isomers of Phenylethynyl. Phenylethyne can undergo homolytic or heterolytic C–H bond fission at the different aromatic C–H bonds as well as at the ethynyl C–H bond. The phenylethynyl radical is formed when the ethynyl bond breaks homolytically. When an aromatic C–H bond is broken, the isomer formed is either (a) *ortho*-ethynylphenyl, (b) *meta*-ethynylphenyl, or (c) *para*-ethynylphenyl.

Figures 2 and 3 show the optimized geometries of the radicals and anions of these three isomers, respectively. The geometries of the *ortho*- and *meta*-ethynylphenyl radicals and anions necessarily optimize to C_s symmetry. The *para*-ethynylphenyl radical and anions take on C_{2v} equilibrium geometries. The bond lengths in the ethynylphenyl radicals are longer according to B3LYP than those for MP2 using the DZP++ basis set (Figure 2). The discrepancy between the two is as large as 0.002 Å for C–H bonds and 0.042 Å for C–C bonds. While the DFT bond

lengths are shorter than those predicted by MP2 for the neutral compound, this trend is reversed for the anion. Perhaps this is a consequence of the extra correlation introduced upon binding the electron; it is well-known that MP2 typically overestimates correlation and that correlation usually increases bond lengths, particularly where multiple bonds are present.^{41,42} Further, the C≡C bond length is shorter in the anion.

An interesting feature observed in the phenyl ring involves the bond angles at the radical carbon atoms. In the radicals, the bond angle is $\sim 126^\circ$ whereas in the anions, much smaller bond angles are predicted ($\sim 112^\circ$). This can be rationalized by considering the extra repulsion introduced by binding the electron, that is, valence shell electron pair repulsion theory (VSEPR) predicts this trend.

The relative energies of the *ortho*-, *meta*-, and *para*-ethynylphenyl are difficult to pinpoint. B3LYP//DZP++ gives the relative energies as (1.00, 0.00, 0.21) kcal/mol, respectively, which is in spectacularly good agreement with the corresponding CCSD(T)/cc-pVQZ//B3LYP/DZP++ values of (1.00, 0.00,

TABLE 4: Adiabatic Electron Affinities (EA_{ad}), Bond Dissociation Energies (BDE), and Proton Affinities (PA) of Phenylethynyl, *ortho*-, *meta*-, and *para*-ethynylphenyl, and Phenylethyne (phenylacetylene)^a

		Methods	
		B3LYP/DZP++	CCSD(T)/DZP++/ MP2/DZP++
phenylethynyl			
electron affinity (eV)	3.00 (3.00)		3.03
BDE (kcal/mol) ^b	128.8		134.3
PA _{ad} (kcal/mol) ^c	374.7		377.7
ethynylphenyl			
<i>ortho</i> - electron affinity (eV)	1.39 (1.45)		1.50
BDE (kcal/mol) ^b	118.3		124.4
PA _{ad} (kcal/mol) ^c	401.3		403.1
<i>meta</i> - electron affinity (eV)	1.34 (1.40)		1.43
BDE (kcal/mol) ^b	117.3		123.4
PA _{ad} (kcal/mol) ^c	401.3		403.8
<i>para</i> - electron affinity (eV)	1.38 (1.43)		1.54
BDE (kcal/mol) ^b	117.5		125.8
PA _{ad} (kcal/mol) ^c	400.7		403.5
phenylethyne			
electron affinity (eV)	-0.18 (-0.05)		-0.95

^a Zero-point vibrationally corrected values of EA_{ad} are in parentheses.

^b BDE are the bond dissociation energies required to break a C–H bond in phenylethyne to form the respective radicals. ^c The proton affinities are the free energy changes when the title anion accepts a proton. Note: The total energies for the hydrogen atom are -0.50191 Hartrees (B3LYP/DZP++) and -0.49929 Hartrees (MP2/DZP++).

0.09) kcal/mol. However, these energy differences are too small to definitively assign the global minimum. The *meta*-ethynylphenyl radical lies 11.5 kcal/mol below the ²B₁ state of the phenylethynyl radical; this increases to a more sizable 17.8 kcal/mol at the CCSD(T)/cc-pVQZ//B3LYP/DZP++ level of theory. Such a change in energetics, coupled with the previous observations in the ²B₁ – ²A₁ states of the phenylethynyl radical, suggests that DFT preferentially stabilizes phenylethynyl's π states.

The adiabatic electron affinities for the *o*-, *m*-, and *p*-ethynylphenyl radicals are very similar, taking values of 1.39, 1.34, and 1.38 eV (B3LYP/DZP++), respectively (Table 4). The radicals are stabilized by hyperconjugation, which results from the interaction of the electrons of the adjacent sigma C–H bonds with the singly occupied molecular orbital. This is the

cause of the lower electron affinity for the isomers relative to the phenylethynyl radical.

F. Bond Strengths and Proton Affinities. Thermochemical data such as the ≡C–H bond strength in phenylethyne and absolute proton affinities of the phenylethynyl and ethynylphenyl anions have been predicted in the gas phase (298 K) with the B3LYP/DZP++ and CCSD(T)/DZP++//MP2/DZP++ methods (Table 4). The theoretical bond dissociation energies are determined from the energy differences between the neutral radical and phenylethyne.



$$D(\text{PhCC-H}) = E(\text{PhCC}\cdot) + E(\text{H}\cdot) - E(\text{PhCCH}) \quad (8)$$

The bond dissociation energy for the ethynyl C–H bond in phenylethyne is predicted to be 128.8 kcal/mol (B3LYP/DZP++), which is in accord with literature values.^{9,27} However, the CCSD(T)/DZP++//MP2/DZP++ method predicts a slightly higher value for the C–H dissociation energy (134.3 kcal/mol) in this case. The latter error is due to the spin contamination $\langle S^2 \rangle = 1.23$ in the UHF wave function for the phenylethynyl radical.

From eq 6, the electron affinity of the neutral species depends on the bond dissociation energy. If the bond dissociation energy predicted for the C–H bond with the above method is considered (128.8 kcal/mol), then the electron affinity of the PhCC radical is estimated to be 3.06 eV.

The adiabatic proton affinity (PA_{ad}) of the phenylethynyl anion is determined as the difference between the energies of the anion and the neutral phenylethyne.



$$\text{PA}_{\text{ad}} = E(\text{PhCC}^-) - E(\text{PhCCH}) \quad (10)$$

Table 4 also reports the proton affinities of the ethynylphenyl anions. As expected, the proton affinities of the *o*-, *m*-, and *p*-ethynylphenyl anions are higher than that of the phenylethynyl anion. The high proton affinities of the *o*-, *m*-, and *p*-ethynylphenyl anions are observed due to the involvement of the sp² hybridized aromatic carbon center.

However, the aromatic C–H bond dissociation energies are lower (~10 kcal/mol) than that of the ethynyl C–H bond (Table

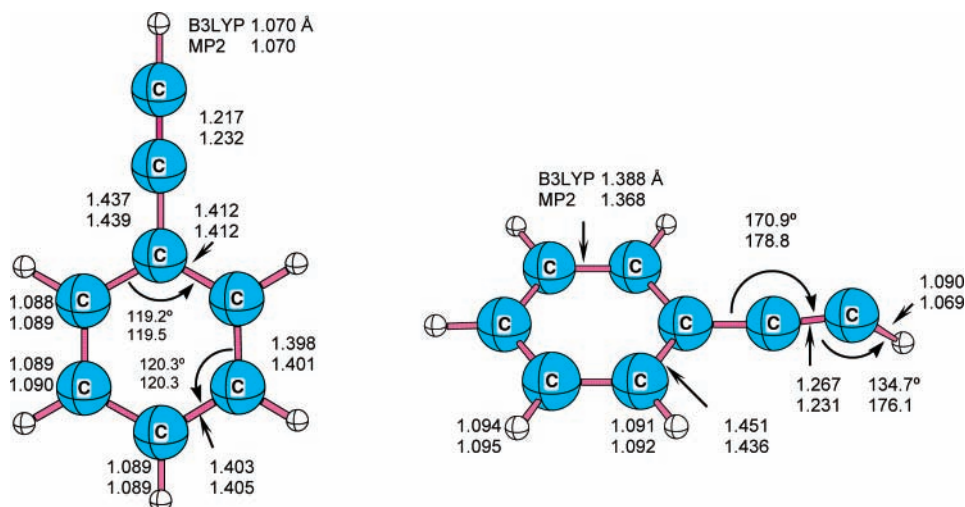


Figure 4. Optimized geometry of phenylethyne (phenylacetylene) and its radical anion predicted by the B3LYP/DZP++ and MP2/DZP++ methods. The ground state of phenylethyne has C_{2v} symmetry (¹A₁). The optimized structure of the phenylethyne radical anion is predicted to have C_s (²A') symmetry with the B3LYP/DZP++ and MP2/DZP++ methods.

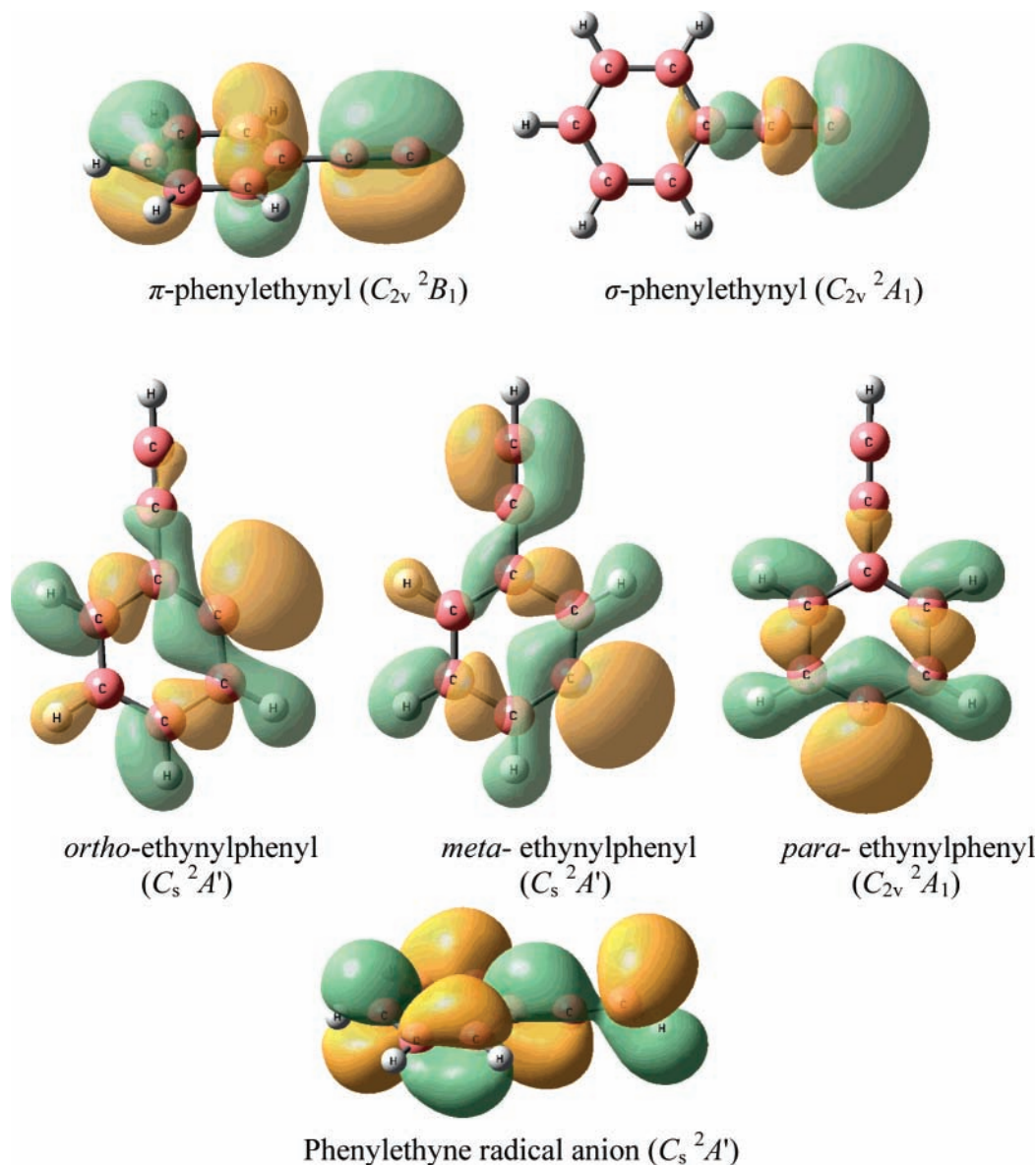


Figure 5. Qualitative molecular orbital diagrams of the singly occupied molecular orbitals of the phenylethynyl radicals, its isomers, and the phenylethynyl radical anion at the respective B3LYP/DZP++ optimized geometries.

4). This result may be understood in light of the shorter ethynyl C–H bond (Figure 4).

Figure 4 shows the optimized structures of phenylethyne and its radical anion predicted by the B3LYP/DZP++ and MP2/DZP++ methods. The phenylethynyl radical anion is formed when phenylethyne accepts an electron in the gas phase. The adiabatic electron affinity predicted by the B3LYP/DZP++ method is -0.18 eV, which depicts phenylethyne as a very poor electron acceptor in the gas phase. Scheer and Burrow reported a vertical electron affinity value for phenylethyne to be -0.35 eV,³¹ with a smaller basis set (B3LYP/6-31G(d)).

G. Vibrational Frequencies. The harmonic vibrational frequencies of the $3N-6$ modes of vibration ($N = 13$) for the phenylethynyl radical and its anion predicted by the B3LYP/DZP++ method are available as the supporting material. The active infrared vibrational modes in the radical and anion are of A_1 , B_1 , and B_2 symmetries.

The fundamental infrared stretching frequencies associated with a C≡C triple bond lie typically in the range 2250 – 2100 cm^{-1} . The harmonic stretching frequency of the C≡C bond ($r_e = 1.217$ Å) in phenylethyne (PhC≡CH) is predicted to lie

around 2185 cm^{-1} . However, the stretching frequencies for ethynyl C≡C bond in the radical and anion are 1966 and 2032 cm^{-1} , respectively. The lower frequencies associated with the stretching frequencies of the ethynyl C≡C bonds in the radical and anion with respect to that in the phenylethyne reflect the lengthening (0.03 Å) in the ethynyl bond ($r_e\text{C}\equiv\text{C}(\text{radical}) = 1.290$ Å; $r_e\text{C}\equiv\text{C}(\text{anion}) = 1.261$ Å).

The imaginary vibration frequencies predicted for the C_{2v} radical (transition state) by the errant BLYP, BP86, BPW91, and B3PW91 functionals are unreasonably high. The high imaginary C–C≡C bending frequency is associated with symmetry breaking from C_{2v} to C_s geometry.⁴³ Since the true equilibrium geometry of the phenylethynyl radical is of C_{2v} symmetry, one need not be concerned about this spurious vibrational frequency.

The harmonic vibrational frequencies corresponding to the equilibrium geometries of the *o*-, *m*-, and *p*-ethynylphenyl radicals and anions (B3LYP/DZP++ method) are also provided as supplementary data. The IR frequencies associated with the C≡C triple bonds in the radicals are in the range 2191 – 2183 cm^{-1} .

H. Molecular Orbitals. The singly occupied molecular orbital (B3LYP/DZP++) plots of the phenylethynyl radical and its isomers are presented in Figure 5. As discussed above, the phenylethynyl radical is seen to be a π radical. However, the *o*-, *m*-, and *p*-ethynylphenyl radicals are clearly σ radicals from the orbital pictures.

IV. Summary and Conclusions

The phenylethynyl radical is predicted to lie 10.5, 11.5, and 11.3 kcal/mol higher than the *o*-, *m*-, and *p*-ethynylphenyl radicals, respectively, at the B3LYP/DZP++ level of theory. These values increase to 18.6, 17.8, and 27.0 kcal/mol, respectively, upon the introduction of single-point energies at the CCSD(T)/cc-pVQZ level, showing an artificial stabilization of the phenylethynyl radical present in the DFT calculations. However, the phenylethynyl radical is significantly higher in energy than the ethynylphenyl radicals at all levels of theory. The energetic trends associated with these radicals are mainly due to resonance stabilization. Since the *o*-, *m*-, and *p*-ethynylphenyl radicals are σ radicals, the electron densities in their π networks are much higher than that of the phenylethynyl radical. As a result, the isomers of phenylethynyl are more resonance favored due to their electron-rich π networks.

The electron affinities of the *o*-, *m*-, and *p*-ethynylphenyl radicals are much lower than that of phenylethynyl. Since these three σ radicals are already resonance stabilized, the energy differences between the radicals and their respective anions are lower compared to that with the phenylethynyl radical. The latter species, of C_{2v} symmetry, is a π radical in its electronic ground state and has a predicted adiabatic electron affinity of 3.00 eV.

The energetic range between the BDEs of the *o*-, *m*-, and *p*-ethynylphenyl radicals is only 0.8–1.0 kcal/mol. The ethynyl C–H bond energy differs by ca. 10 kcal/mol from those of the aromatic C–H bonds. Although these hydrocarbons have high C–H bond energies, the formation of the *o*-, *m*-, and *p*-ethynylphenyl radicals in pyrolysis reactions or at high temperature is more feasible than the formation of the phenylethynyl radical.

The cleavage of the σ ethynyl C–H bond in phenylethyne yields a σ radical, which is energetically disfavored with respect to the π radical. This present research provides evidence that the theoretical energy separation ($\Delta E_{\sigma-\pi}$) between the ground phenylethynyl π radical and its σ radical is 10.1 kcal/mol (B3LYP/DZP++). In contrast, the energy separations $\Delta E_{\sigma-\pi}$ between the ground σ radicals of the *o*-, *m*-, and *p*-ethynylphenyl and their corresponding π radicals are –46.4, –51.8, and –47.7 kcal/mol (B3LYP/DZP++), respectively.

Acknowledgment. R.K.S. wishes to thank the Center for Computational Chemistry and the Research Computing Center at the University of Georgia for facilitating this work. The research has been supported by the U.S. Department of Energy, Basic Energy Sciences, Combustion Research program, and by the Tertiary Education Commission (TEC) of Mauritius. The Berkeley NERSC supercomputing facility of the U.S. Department of Energy was instrumental in computing the perturbation theory and coupled-cluster results described herein.

Supporting Information Available: Molecular orbitals of C_s phenylethynyl, Cartesian coordinates of the σ radicals of phenylethynyl, and IR vibrational frequencies predicted by the MP2 and B3LYP methods with the DZP++ basis set for the isomers of phenylethynyl are given. Energy separations $\Delta E_{\sigma-\pi}$

between the ground σ radicals of the *o*-, *m*-, and *p*-ethynylphenyl and their corresponding π radicals predicted by the B3LYP/DZP++ method are also presented. This material is available free of charge via the Internet at <http://pubs.acs.org>.

References and Notes

- (1) Coleman, J. S.; Hudson, A.; Root, K. D. J.; Walton, D. R. M. *Chem. Phys. Lett.* **1971**, *11*, 300.
- (2) Kasai, P. H.; McBay, H. C. *J. Phys. Chem.* **1984**, *88*, 5932.
- (3) Easley, W. C.; Weltner, W. *J. Chem. Phys.* **1970**, *52*, 197.
- (4) Sreeruttun, R. K.; Ramasami, P.; Wannere, C. S.; Paul, A.; Schleyer, P. v. R.; Schaefer, H. F. *J. Org. Chem.* **2005**, *70*, 8676.
- (5) Martelli, G.; Spagnolo, P.; Tiecco, M. *J. Chem. Soc. B: Phys. Org.* **1970**, 1413.
- (6) Casanova, J.; Geisel, M.; Morris, R. N. *J. Am. Chem. Soc.* **1969**, *91*, 2156.
- (7) Bölm, S.; Páfk, P.; Exner, O. *New J. Chem.* **2006**, *30*, 384.
- (8) Exner, O. *Prog. Phys. Org. Chem.* **1990**, *18*, 129.
- (9) Palat, K.; Bölm, S.; Braunerova, G.; Waissner, K.; Exner, O. *New J. Chem.* **2002**, *26*, 861.
- (10) Hofmann, J.; Zimmermann, G.; Guthier, K.; Hebgen, P.; Homann, K.-H. *Liebigs Ann. Chem.* **1995**, 631.
- (11) Gu, X.; Guo, Y.; Zhang, F.; Mebel, A. M.; Kaiser, R. I. *Chem. Phys. Lett.* **2007**, *436*, 7.
- (12) Rienstra-Kiracofe, J. C.; Tschumper, G. S.; Schaefer, H. F.; Nandi, S.; Ellison, G. B. *Chem. Rev.* **2002**, *102*, 231.
- (13) Becke, A. D. *Phys. Rev. A* **1988**, *38*, 3098.
- (14) Becke, A. D. *J. Chem. Phys.* **1993**, *98*, 1372.
- (15) Lee, C.; Yang, W.; Parr, R. G. *Phys. Rev. B* **1988**, *37*, 785.
- (16) Perdew, J. P. *Phys. Rev. B* **1986**, *33*, 8822.
- (17) Becke, A. D. *J. Chem. Phys.* **1993**, *98*, 5648.
- (18) Dunning, T. H.; Hay, P. J. In *Modern Theoretical Chemistry*; Schaefer, H. F., Ed.; Plenum: New York, 1977; Vol. 3, pp 1–27.
- (19) Huzinaga, S. *J. Chem. Phys.* **1965**, *42*, 1293.
- (20) Huzinaga, S. *Approximate Atomic Wavefunctions II*; University of Alberta: Edmonton, Alberta, 1971.
- (21) Lee, T. J.; Schaefer, H. F. *J. Chem. Phys.* **1985**, *83*, 1784.
- (22) Murray, C. M.; Davidson, E. R. *Chem. Phys. Lett.* **1991**, *187*, 451.
- (23) Lee, T. J.; Jayatilaka, D. *Chem. Phys. Lett.* **1993**, *201*, 1.
- (24) Crawford, T. D.; Schaefer, H. F.; Lee, T. J. *J. Chem. Phys.* **1996**, *105*, 1060.
- (25) Dunning, T. H. *J. Chem. Phys.* **1989**, *90*, 1007.
- (26) Kendall, R. A.; Dunning, T. H.; Harrison, R. J. *J. Chem. Phys.* **1992**, *96*, 6796.
- (27) Woon, D. E.; Dunning, T. H. *J. Chem. Phys.* **1993**, *98*, 1358.
- (28) Frisch, M. J.; et al. *Gaussian94*, revision E.2; Gaussian Inc: Pittsburgh, PA, 1995.
- (29) Frisch, M. J.; et al. *Gaussian03*, revision C.02; Gaussian Inc: Wallingford, CT, 2004.
- (30) *The Massively Parallel Quantum Chemistry Program (MPQC)*, version 2.3.1; Curtis L. Janssen, Ida B. Nielsen, Matthew L. Leininger, Edward F. Valeev, Edward T. Seidl; Sandia National Laboratories: Livermore, CA, 2004.
- (31) *MOLPRO* is a package of ab initio programs written by H.-J. Werner, P. J. Knowles, R. Lindh, F. R. Manby, M. Schütz, P. Celani, T. Korona, G. Rauhut, R. D. Amos, A. Bernhardsson, A. Berning, D. L. Cooper, M. J. O. Deegan, A. J. Dobbyn, F. Eckert, C. Hampel, G. Hetzer, A. W. Lloyd, S. J. McNicholas, W. Meyer, M. E. Mura, A. Nicklaß, P. Palmieri, R. Pitzer, U. Schumann, H. Stoll, A. J. Stone, R. Tarroni, and T. Thorsteinsson.
- (32) Sreeruttun, R. K.; Ramasami, P.; Yan, G.; Wannere, C. S.; Schleyer, P. V.; Schaefer, H. F. *Int. J. Mass Spectrom.* **2005**, *241*, 295.
- (33) Ervin, K. M.; Lineberger, W. C. *J. Phys. Chem.* **1991**, *95*, 1167.
- (34) Bartmess, J. E.; Scott, J. A.; McIver, R. T. *J. Am. Chem. Soc.* **1979**, *101*, 6046.
- (35) Chabincyn, M. L.; Brauman, J. I. *J. Am. Chem. Soc.* **2000**, *122*, 8739.
- (36) Fulton, J. R.; Sklenak, S.; Bouwkamp, M. W.; Bergman, R. G. *J. Am. Chem. Soc.* **2002**, *124*, 4722.
- (37) Blanksby, S. J.; Ellison, G. B. *Acc. Chem. Res.* **2003**, *36*, 255.
- (38) Curl, R. F.; Carrick, P. G.; Merer, A. J. *J. Chem. Phys.* **1985**, *82*, 3479.
- (39) Serrano-Andrés, L.; Merchán, M.; Jabłoński, M. *J. Chem. Phys.* **2003**, *119*, 4294.
- (40) Scheer, A. M.; Burrow, P. D. *J. Phys. Chem. B* **2006**, *110*, 17751.
- (41) DeFrees, D. J.; Levi, B. A.; Pollack, S. K.; Hehre, W. J.; Binkley, J. S.; Pople, J. A. *J. Am. Chem. Soc.* **1979**, *101*, 4085.
- (42) Ramos, M. N.; Lopes, K. C.; Tavares, A. M.; Ventura, E.; do Monte, S.; Araújo, C. M. U. R. *J. Mol. Struct.* **2006**, *758*, 253.
- (43) Allen, W. D.; Horner, A. D.; DeKock, R. L.; Remington, R. B.; Schaefer, H. F. *Chem. Phys.* **1989**, *133*, 11.